



## Land Cover Classification and Monitoring: the STEM Open Source Solution

**Francesco Nex<sup>1,5\*</sup>, Luca Delucchi<sup>2</sup>, Damiano Gianelle<sup>3,4</sup>, Markus Neteler<sup>2</sup>,  
Fabio Remondino<sup>1</sup> and Michele Dalponte<sup>3</sup>**

<sup>1</sup>Fondazione Bruno Kessler, 3D Optical Metrology Unit, Via Sommarive 18, 38123 Trento, Italy

<sup>2</sup>Fondazione Edmund Mach, Biodiversity and Molecular Ecology Department,  
Via E. Mach 1, 38010 San Michele all'Adige, Italy

<sup>3</sup>Fondazione Edmund Mach, Sustainable Agro-ecosystems and Bioresources Department,  
Research and Innovation Centre, 38010 Via E. Mach 1, San Michele all'Adige, Italy

<sup>4</sup>Fondazione Edmund Mach, FoxLab, Joint CNR-FEM Initiative,  
Via E. Mach 1, 38010, San Michele all'Adige (TN), Italy

<sup>5</sup>University of Twente, ITC Faculty, EOS Department,  
Hengelosestraat 99, 7514 AE, Enschede, The Netherlands

\*Corresponding author, e-mail address: f.nex@utwente.nl

### Abstract

Agricultural and forest monitoring is a valued instrument needed by public authorities (PA) for determining land uses, planning natural resources management and collecting taxes. Remote Sensing (RS) can provide accurate information over large areas and it has been already widely used for these tasks. Orthophotos and LiDAR data are regularly acquired to monitor land cover changes in many countries. However, the data processing is usually done through photointerpretation and PA are lacking an automated software for this task. The STEM project aimed at the development of an open source software to process RS data for agricultural and forests monitoring. The developed plug-in can be used by inexperienced users to monitor large land covers. In the paper the main software functionalities are described, with particular emphasis on the most innovative modules and algorithms. Some results obtained by these modules are shown as well to demonstrate the efficiency and reliability of the plug-in.

**Keywords:** Agriculture, forest, classification, monitoring, open source, public administration.

### Introduction

#### *Background*

Land covers monitoring is an important issue for public administrations all over the world. In the European context, agricultural and forest land cover monitoring are considered particularly important as the precise knowledge about crop and forest extension, typology and health condition, plays a relevant role for economic and environmental purposes.

Agricultural monitoring is a relevant instrument needed by public authorities for determining the current land use, planning efficient land management practices of rural areas and collecting taxes. A better management of natural sources is also requested by the European Community policies [Bignal, 1998]. For these reasons, each European country is asked to have reliable and always up-to-date information about the crop extensions in its territories. In the same way, forests cover 44% of the European territory, and they represent in some countries a large share of their gross domestic product. Although in many countries forests are privately owned, public administrations are in charge of their monitoring. National Forest Inventories are carried out at regular intervals to know the qualitative (e.g. species, structure) and quantitative (e.g. volume, basal area) attributes of forests. These inventories are related not only to forest economical exploitation but also to the knowledge of forest biomass required by international environmental protocols as related to the carbon stored by the trees. Moreover it is extremely important to have detailed knowledge of forests in order to preserve their ecological biodiversity.

Among the available technologies, Remote Sensing (RS) has become an asset in the repeated and cost-effective investigation of the land use over large areas (regional and national level). RS techniques have been greatly improved in the last two decades thanks to the development of more efficient algorithms for the classification and feature extraction from images and point clouds: reliable thematic classifications are provided by using satellite and aerial (multi- and hyper-spectral) images as input [Warner and Steinmaus, 2005; Bruzzone and Carlin, 2006; Nemmour et al., 2006; Helmholtz et al., 2014], while tridimensional investigations about volumes and surfaces can be performed thanks to Light Detection And Ranging (LiDAR) data or photogrammetric point clouds [Pirotti et al., 2012].

All these data have become a valuable source for land administrators to extract quantitative information at a sustainable price and with high repeatability. Indeed many public authorities have settled programs of regular data acquisition at national and regional level, and nowadays almost in every EU country there is a time repeated acquisition of remote sensing data, often using both passive and active sensors. Regarding the imagery the most common products used are ortho-images acquired using 3-4 spectral bands cameras, and sub-meter resolution (i.e. the AGEA flight in Italy, D. Lgs. May 27<sup>th</sup> 1999). These data are usually used to make land cover maps through photo-interpretation, and they are mainly adopted for urban and agricultural monitoring. Many countries has more recently started to acquire LiDAR data over their territories, to generate accurate digital surface models (DSM) and Digital Terrain Models (DTM) as well as to monitor large forest areas.

However, this information is just getting partially exploited by public administrations due to the enormous size of the collected data and the limited performance of the hardware commonly available that would require very long processing times. Moreover, data processing performed using proprietary software can lead to unsustainable costs.

Most of the currently available RS software packages do not process both images and LiDAR point clouds together. They usually offer broad tools for image processing without providing straightforward and turn-key workflows for specific tasks (such as crop monitoring). Thus, experienced users are needed to perform the complete processing even if RS expertise is quite uncommon in many public administrations and high automation as well as user-friendliness of the software are strictly required to process huge amount of data.

## The STEM Project

The STEM (*Sistema di telerilevamento e di monitoraggio del territorio e dell'ambiente Trentino*) project, funded by the Autonomous Province of Trento (Italy), aims at implementing algorithms and tools for the efficient processing of RS data for agricultural and forestry applications. The algorithms are integrated in a dedicated plug-in that enables users to process data from the input stage (image and LiDAR data) to the final delivered thematic maps. In the last decade, the use of open source solutions became an important asset to reduce costs and improve the efficiency of many public administrations all over Europe (Joinup Platform, available online at: <https://joinup.ec.europa.eu/>, last accessed on October 15<sup>th</sup> 2015). This trend has been further pushed by the inception of the economic crisis in the very last years. For these reasons, the developed algorithms have been integrated in the free and open source QGIS (<http://www.qgis.org/>) software using an ad-hoc plug-in. External free and open source libraries as well as in-house algorithms, have been integrated in the plug-in to fulfil all the required functionalities of the system. All the algorithms have been developed and optimized in order to use the available data as input and to prevent the additional costs of further data acquisitions. In any case, the tool is data independent and different types of data can be processed as well. Supervised classification algorithms and well-tested state-of-the-art procedures have been chosen when possible to assure the maximum reliability and stability of the provided results in every operative condition. Experimental algorithms have been set up to generate new information and thematic maps or to simplify existing tools delivering turn-key solutions for public sector technicians. As the process of huge amount of data can be very time consuming, a dedicated server-client architecture has been developed for the processing of the data in remote. In this paper, the general description of the whole system is firstly given. Then, a description of the main plug-in functionalities and the most significant algorithms is provided. The achieved results on some test sites will be presented too. The paper ends with a critical discussion of the pros and cons of the developed tool and its possible future progresses.

## The STEM plug-in

The STEM plug-in is developed as a QGIS extension. The plug-in is developed in the Python programming language leveraging several open source libraries currently available to analyse geographical data (as shown in Fig. 1) while the Python bindings are used to connect it to the QGIS core application.

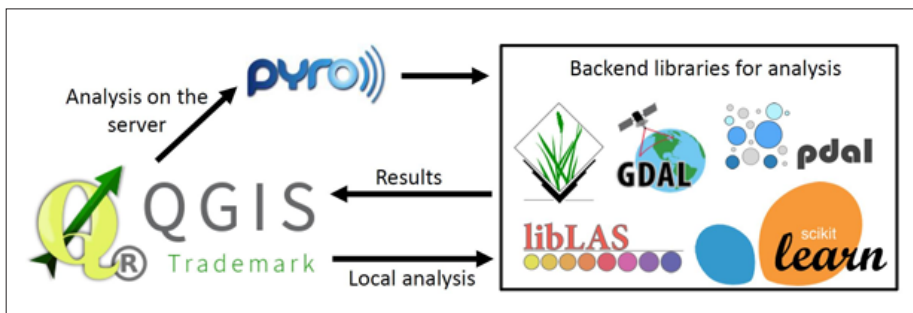
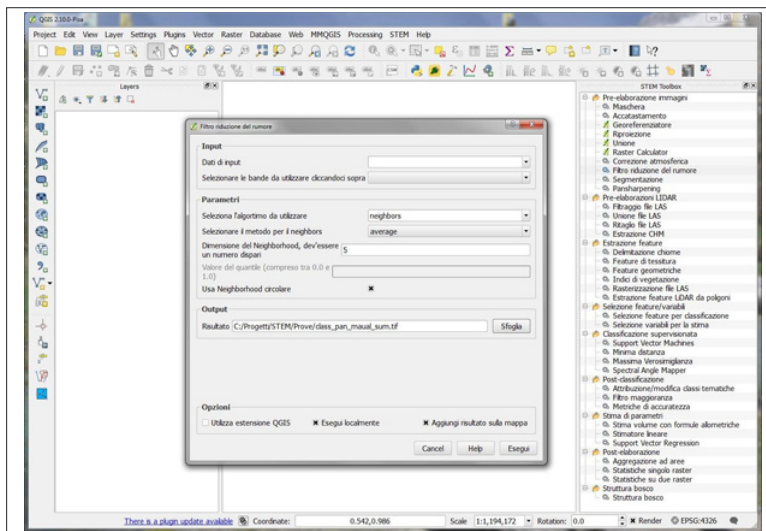


Figure 1 - The general architecture of the STEM plug-in and the used modules.

In particular, geospatial data management and image processing are made possible thanks to the GRASS GIS library (V 7.0) (<http://grass.osgeo.org/>) where more than 400 modules are currently available [Neteler et al., 2012]. The support for geospatial raster and vector file management is provided by the GDAL/OGR (<http://www.gdal.org/>) translator library, while the libLAS (<http://www.liblas.org/>) and PDAL (<http://www.pdal.io/>) libraries are used to process and modify point cloud data. The machine learning algorithms, used in the classification and regression processes, are provided by the Python library scikit-learn (<http://scikit-learn.org/stable/>) while the remaining functionalities are directly incorporated from QGIS.

The big amount of data collected on large areas are usually very difficult to process on a single desktop computer as they require very high performance computing resources. For this reason, the developed plug-in can be connected to external PCs or clusters in order to remotely process the data for the user. The Pyro4 (<http://pythonhosted.org/Pyro4/>) library is used for this connection. This library is a distributed object middleware for Python RPC (Remote Procedure Call) - and works through the remote method invocation technology. Pyro4 allows to receive data from the client and run the analysis on the remote server. Users can easily launch data processing on the remote machines using the plug-in. The remote processing option can be simply selected as an option in the plug-in, without additional efforts for the users. A dedicated interface for batch processes has been developed for the processing of big datasets on the same PC without user interaction too.



**Figure 2 - The STEM plug-in in QGIS (right column) and its window interface. Parameters are initialized by default values. The modules on the right are listed according to the processing steps.**

The STEM plug-in has been developed and tested to run on both Linux and Windows operative systems. The commands line messages and the help text are currently in Italian language, as the initial customer is the Autonomous Province of Trento (Italy) but they will be translated to English in near future. The plug-in is organized according to a sequence of

modules, each of them representing a different step of the workflow. The user can process the data following a sequence of steps as they are presented in the plug-in (Fig. 2). Each module can be set up using a dedicated window interface, where default values are initially displaced.

The modules can be grouped in three main categories as reported in the following sections shown in Figure 3: (i) *general modules*, useful for every kind of application and using both images and LiDAR data as input (red steps), (ii) *agriculture modules*, for the crop monitoring using multispectral images (blue steps), and (iii) *forest modules*, devoted to the extraction of forestry attributes from hyperspectral images and LiDAR data (green steps). Both agriculture and forest modules aim at classifying the land use of the area under analysis. The estimation of some tree attributes (Section Attributes estimation) have been specifically conceived for forest applications. As shown in Figure 3, multispectral images are used for agriculture applications while the use of hyperspectral images has been limited to forest applications so far. Image features are only extracted from multispectral data while spectral information from each band is considered as feature when hyperspectral images are available. LiDAR data processing can be performed considering each tree crown as basic element of the analysis (see section Individual Tree Crowns (ITC) delineation) or adopting user defined polygons. Several LiDAR features can be extracted considering these data in raster format (Section LiDAR features extraction) or as native point clouds (Section Vertical structure of the forest). When both image and LiDAR data are available on the same area, both sets of corresponding features can be processed together as well for classification purposes. Default values has been set-up according to many experimental tests performed on the developed tools.

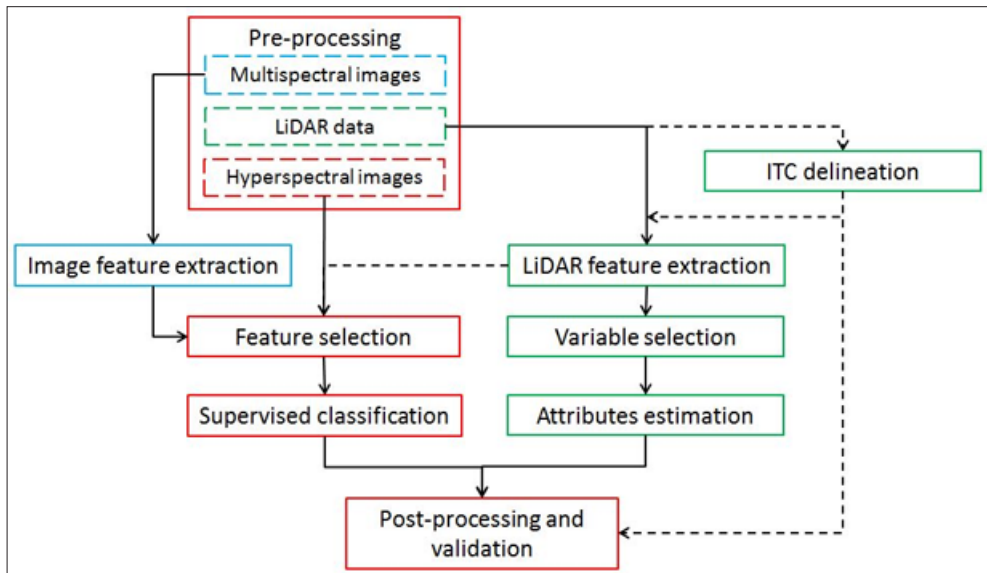


**Figure 3 - General organization of the STEM plug-in: the processing is organized according a sequence of tools. General modules are in red, agriculture modules in blue while forest modules are in green.**

## **STEM General Modules**

### **Pre-processing**

In these modules, algorithms for both image and LiDAR data processing are implemented. Algorithms devoted to geo-referencing, mosaicking, layer stacking, filtering and masking have been implemented to process both satellite and aerial images. Specific algorithms for atmospheric correction (i.e. 6S method) and pansharpening (i.e. Brovey, HIS, PCA) have been realized for satellite image processing.

Filtering, merging, splitting and rasterizing algorithms for LiDAR point clouds have been implemented as well. The normalized Digital Surface Model (nDSM) extraction can be performed exploiting a Digital Terrain Model (DTM) too. The plug-in allows to process and save data as *.las* and *.laz* file.

### **Feature and variable selection**

The most significant features/variables are extracted to speed and improve the classification and the attribute estimation tasks. Feature and variable selection methods usually can be divided into three categories: (i) filter methods; (ii) wrapper methods; and (iii) embedded methods. Filter methods (i) perform the feature/variable selection as a pre-processing step independently of the algorithm used for classification/regression. Wrapper methods (ii) select an optimized set of features/variables for the specific classification/regression technique considered. Embedded methods (iii) incorporate the feature/variable selection step in the training of the algorithm. The STEM toolbox includes one filter method for feature selection and one embedded method for both feature and variable selection.

The filter method is based on the so-called Sequential Forward Floating Selection (SFFS) algorithm [Pudil et al., 1994], and on the Jeffries-Matusita distance (JM) [Bruzzone et al., 1995]. The SFFS method iteratively adds and remove features in order to define a sub-optimal set of features that maximize the Jeffries Matusita distance. This method has been successfully used in other classification studies like Hilker et al. [2005], Dalponte et al. [2008, 2009, 2012].

The wrapper method is the Recursive Feature Elimination (RFE) [Tsai et al., 2012] in combination with the Support Vector Machine (SVM) classifier and the Support Vector Regression (SVR) estimator. This technique performs the selection of a subset of most discriminative/informative features/variables (with predefined cardinality) through a sequential backward elimination procedure guided by the margin maximization principle [Bazi et al., 2006]. Its recursive procedure requires training a SVM/SVR with the current set of features/variables and removing at each iteration the feature/variables that least decreases the margin until the desired number of features/variables is reached [Bazi et al., 2006].

### **Supervised classification**

Four classification algorithms are implemented in the plug-in: (i) Gaussian Maximum Likelihood (GML); (ii) k-Nearest Neighbour (kNN); (iii) Spectral Angle Mapper (SAM); and (iv) Support Vector Machines (SVM). All these methods can take as input both image and LiDAR features.

The GML [Hoffbeck and Landgrebe, 1996] is a parametric classifier based on the Bayesian decision theory. It assumes that the training statistics for each class have a normal distribution. The statistics mean vectors and the covariance matrices are used to compute a probability



value to determine whether a pixel belongs to a particular class.

The k-NN [Altman, 1992] is a non-parametric classifier where a set of training samples is mapped in the feature space according to their values. The decision on the class membership of an unlabelled sample is made through a majority vote of its neighbours, with the sample being assigned to the most common class among its k nearest neighbours (k is a positive integer, typically small). The k-NN algorithm is among the simplest of all machine learning algorithms.

The SAM classifier [Kruse et al., 1993] is a physically-based spectral classification that uses an n-D angle to match samples to reference spectra. The algorithm determines the spectral similarity between two spectra by calculating the angle between the spectra and treating them as vectors in a space with dimensionality equal to the number of bands.

The SVM classifier [Vapnik, 1998] is a non-parametric distribution-free classifier. The rationale of this classifier is to implicitly map the original feature space into a space with a higher dimensionality, where classes can be modelled to be linearly separable. This transformation is implicitly performed by applying kernel functions to the original data. The learning of the classifier is associated with a constrained optimization process that is associated with a complex cost function.

### **Post-processing and validation**

Two post-processing methods are implemented in the STEM plug-in:

- i) a spatial filtering that can be applied to the classified image. The spatial filtering is based on a majority rule applied inside a moving window of size defined by the user;
- ii) a classification or an estimation map that can be also aggregated in areas using a shapefile: pixels/ITCs are aggregated according to a statistic chosen by the user (e.g. majority rule in case of classified images, or sum in case of the estimation of volume at ITC level) inside each polygons.

Different validation methods such as the cross-validation and leave-one-out validation have been implemented in the learning phase of the classifiers and of the estimators. A post learning validation is also possible using a separate validation set provided by the user. In each classification validation, the metrics computed are the confusion matrix, the overall accuracy, the kappa accuracy, the producer's and user's accuracies, while the metrics computed for the estimators are the squared correlation coefficient ( $R^2$ ) and the root mean squared error (RMSE).

### ***STEM Agriculture Module***

This module has been mainly conceived for the multi-spectral image processing even if the use of hyperspectral images would be possible as well. In particular, the default parameters have been optimized to provide reliable results on medium resolution aerial images.

### **Image features extraction**

Feature extraction represents the fundamental step for any classification algorithm [Blaschke, 2010]. A large number of features have been presented in the last two decades in both the remote sensing and computer vision literatures. They can be divided in (i) spectral, (ii) textural, (iii) structural, and (iv) geometric features [Helmholz et al., 2014].

Spectral features (i) consider only the spectral information of different bands, often computing

local statistical values (i.e. mean, standard deviation) on a moving window around each pixel. They can be useful when multi-temporal data are considered in the vegetation classification due to the ever-changing colours. Textural features (ii) describe the spatial distribution of tonal variations within a band [Haralick et al., 1973; Amadasun and King, 1989]. Finally structural and geometrical (often grouped in a unique category called contextual) features (iii) describe the size, shape and location of each segmented region that is visible on the image [Trias-Sanz, 2006]. In general, the combination of two or more types of features for agricultural purposes has shown to overcome the results achievable using one separate typology of features [Peled and Gilichinsky, 2010]. For this reason, spectral, textural and contextual features have been combined together in the development of the STEM plug-in.

*Textural features* (i) are computed directly analysing the spectral information of a pixel on all the available bands (the HSV colour space have been adopted) and its adaptive neighborhood at different levels. Most of Haralick's features [Haralick, 1979] have been implemented in the STEM plug-in, even if satisfactory results have been achieved using a limited number of these features. In particular, the default setting considers just the following features: Contrast, Correlation, Entropy, Sum Entropy, Sum Average, Variance, Sum Variance, and Measure of Correlation 1. These features have already shown to be effective [Warner and Steinmaus, 2005] when image structure is regular such as regular spacing in the row orchards, and they are conditioned by the moving windows size employed to determine their values. From experimental tests, a moving window of 7 x 7 pixels size has been considered for this task. Considering ground sampling distances (GSD) dimensions ranging from 0.4 to 0.6 m, this dimension corresponds to 3-4 m on the ground allowing to capture two adjacent rows of the same orchard.

Textural features do not provide any information about the spatial context of pixels [Warner and Steinmaus, 2005]. *Contextual features* (iii) allow to face this kind of problems providing information of region achieved by a segmentation process. However, different segmentation thresholds provide different regions, leading to completely different results. For these reasons, a multi-resolution segmentation approach has been developed. Images are segmented using different values of aggregation in a bottom-up region merging process. At each level, pixels are clustered each other varying the parameters that determine the homogeneity rules in the aggregation process. The contextual analysis of neighbouring regions at the same level or at different levels defines the relation between each pixel spatial context at the same or at different levels [Bruzzone and Carlin, 2006].

The homogeneity rule used in the aggregation takes into account both spectral and spatial constraints. The aggregation distance is first computed using spectral information. Then, two regions are merged together considering both the spectral and compactness information of the regions [Shakelford and Davies, 2003]. The compactness index is defined by the ratio "perimeter/square root of the area". The weight between spectral and geometric components is set to provide more weight to the spectral component.

Considering aerial/satellite images with a 0.5 m GSD resolution and the crop monitoring task, seven different resolution levels have shown to describe in an exhaustive way the pixels relations. As suggested in [Bouman et al., 1994; Bruzzone and Carlin, 2006], the comparison between the mean size of the regions in the image with the average size of the objects in the scene, can provide an empirical indication about the threshold to be used as starting value, while the highest threshold of segmentation should still allow to



distinguish regions characterized by completely different spectral contents (such as roads and grasslands).

The multi-level segmentation process is repeated for all the available bands. On each region, the developed system allows to compute statistical values such as mean, standard deviation and higher order-statistics of both *spectral* and *textural* features. These values are assigned as features to pixels defining that segmented region.

### **STEM Forest Module**

This module can be used to classify or determine attributes on forests. The analysis can be performed on each tree (see following section) or at area level [Corona et al., 2012] using both hyperspectral images and LiDAR data as input.

### **Individual Tree Crowns (ITC) delineation**

The ITC delineation module uses an algorithm based on both a raster canopy height model (CHM) and the raw ALS points cloud that came out among the best in a benchmark study comparing delineation methods across 18 sites in the Alps (method 2 in Eysn et al. [2015]).

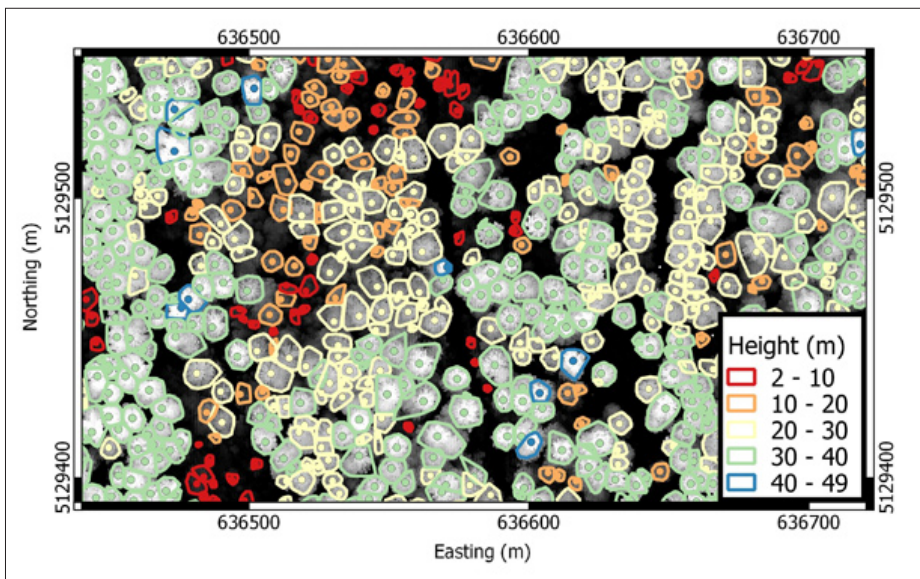


**Figure 4 - Example of the result of the ITC delineation: shapefile polygon of the ITC and location of the tree top with the indication of the tree height.**

The ITC delineation approach finds local maxima within a rasterized CHM, designates these as tree tops, then uses a decision tree method to grow individual crowns around the local maxima. The approach goes through the following steps: (i) a low-pass filter is applied to the rasterized CHM to smooth the surface and reduce the number of local maxima; (ii) local maxima are located using a circular moving window; a pixel of the CHM is labelled as local maxima if its  $z$  value is greater than all other  $z$  values in the window, provided that  $z$  is greater than some minimum height above-ground; (iii) each local maximum is

labelled as an “initial region” around which a tree crown can grow; the heights of the four neighbouring pixels are extracted from the CHM and these pixels are added to the region if their vertical distance from the local maximum is less than some user-defined percentage of the local-maximum height, and less than some user-defined maximum difference; this procedure is repeated for all the neighbours of cells now included in the region, and the process is repeated until no further pixels are added to the region; (iv) from each region that had been identified, the first-return ALS points are extracted (having first removed low elevation points), (v) a 2D convex hull is applied to these points, and the resulting polygons becomes the final ITCs (see Fig. 4). Note that this process is not completely automatic, as the size of the moving window, the small-tree cut-off height, and the percentage- and absolute-height difference thresholds all need to be set by the user.

### LiDAR feature extraction

The module for the feature extraction from the rasterized LiDAR point cloud works according to two different strategies: (i) features are extracted at pixel level and a multiband raster is produced as output, (ii) features are extracted on regions defined by polygons (generated by users or ITC delineation) and the output is stored on polygonal shapefiles. The features produced in output are summarized in Table 1. These features are widely used in the forest volume, basal area and above-ground biomass estimation [Clementel et al., 2012; Corona et al., 2012]. The percentiles mentioned in Table 1 refer to: 30%, 40%, 90% and 95% by default.

**Table 1 - List of the extracted LiDAR features.**

Feature	Description
$H_{min}$	Minimum value of the Z values of the LiDAR points
$H_{max}$	Maximum value of the Z values of the LiDAR points
$H_{mean}$	Mean value of the Z values of the LiDAR points
$H_{median}$	Median value of the Z values of the LiDAR points
$H_{pNth}$	Nth Percentile value of the Z values of the LiDAR points (i.e. $H_{p90} = 90^{th}$ percentile).
$C_{pNth}$	Canopy densities corresponding to the proportions of LiDAR points above the Nth percentile to total number of points (i.e. $C_{p90} =$ canopy density corresponding to the 90 <sup>th</sup> percentile).
$H_{cv}$	Coefficient of variation
Area	Area of the crown (only for ITC level estimates)

### Attribute estimation

The above mentioned features allow to estimate three different attributes both at ITC and area level: volume, above ground-biomass, diameter at breast height. At the moment in the STEM plug-in two supervised estimators are implemented: (i) ordinary least square (OLS) regression; and (ii) support vector regression (SVR). In the future we plan to add

more estimators exploiting the ones already available in the *scikit-learn* library (e.g. logistic regression, decision trees). The OLS estimates the target variable starting from a set of dependent variables. In greater detail this method assumes that the target value is a linear combination of the input variables, and it estimates the coefficients of the corresponding linear model in order to minimize the residual sum of squares between the observed target in the dataset and the target predicted by the linear approximation. This estimator is the most common estimator used in the forestry domain [e.g. in Næsset et al., 2013].

The SVR estimator [Smola and Schölkopf, 2004] is based on the SVM theory. Instead of minimizing the observed training error, SVR attempts to minimize the generalization error bound to achieve generalized performance. The idea of SVR is based on the computation of a linear regression function in a high dimensional feature space where the input data are mapped via a nonlinear function [Basak et al., 2007]. It has been widely used in recent years for solving estimation problems in many applications and with many kinds of remote sensing data [e.g. Bruzzone and Melgani, 2005; Dalponte et al., 2011].

### Vertical structure of the forest

LiDAR data have been largely used for determining the vertical structure of forests [Zimble et al., 2003; Sherill et al., 2008] and monitoring the trees population. The analysis of vertical structures could be limited to the detection of height profiles shapes [Kimes, et al., 2012] or can try to infer the vertical structure of the forest, detecting forests with different layers and vertical distributions [Zimble et al., 2003] of trees. Although the use of full-waveform information has shown to provide big advantages in the layers detection [Whitehurst et al., 2014], this kind of information is often not available, especially if public administration data are considered as input.

For this reason, the developed algorithm exploits only the multi-echo information, relying on a limited number of echoes (i.e. 4 returns) to infer the structure and aiming at classifying the vertical forest structures in three main typologies of forest: single-layers (trees have similar heights), double-layers (trees are distributed in two layers) and multi-layer (trees height is variable) as shown in Figure 5.

The input LiDAR file is initially normalized using the DTM and lower points (e.g. points with height less than 1 m) are filtered as grass or ground points. The area of interest is divided in cells of 30x30 m size [Zimble et al., 2003] as this dimension assures to get a representative sample of the structure. The algorithm is run independently on each of these cells and it is composed by two main steps: (i) the trees layers detection and (ii) the forest type computation.

In the first step, the forest vertical structure is initially classified in single- and double-layers distributions. To do that, points are grouped in two classes using a k-means algorithm and the distribution of height values on these two clusters are analysed. A vertical structure is classified as double-layer if the following conditions are respected: (a) each cluster must have a minimum percentage of points  $P\%$ ; (b) the difference between the mean height values of the two layers is higher than a threshold  $dH$ ; (c) the lower layer has a minimum percentage of second (third and fourth) return points ( $\%S$ ) and (d) the two layers are well separated as they are both local maxima of the height distribution; (e) local minima must be in between these values and the ratio between local maxima and local minima is considered as parameter ( $rM$ ). If a candidate double-layer structure does not satisfy these conditions,

the corresponding cell is classified as single-layer.

In the step (ii) the presence of multi-layer vertical structures is considered as well, evaluating the compactness of the detected layer(s). To do that, the four returns are considered and their distribution in  $Z$  is analysed to assess the compactness of the vegetation: returns close to each other statistically means that a compact layer can be detected in the vegetation, while the structure is classified as multi-layer when returns have higher differences in height. In this case, two new parameters are considered: the distance between the first and the last return ( $f$ ) and the height difference between the first two and the last two returns ( $g$ ). When ( $f$ ) is lower than a threshold ( $dt$ ), the structure can be only single-layer, while when the parameter ( $g$ ) is higher than a threshold ( $mD$ ), the structure is always classified as multi-layer.

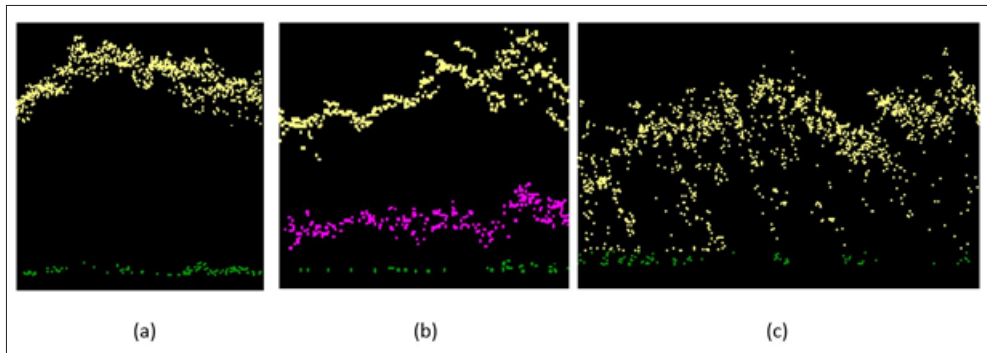


**Figure 5 - Example point cloud in a (a) single-, (b) double- and (c) multi-layer forest vertical structure.**

The above mentioned thresholds influence the results achieved in the classification. Anyway, the following set of parameters has shown to provide satisfying results in very different areas considered in the performed tests:  $\%P=15\%$ ,  $dH=5$  m;  $\%S=20\%$ ;  $rM=0.5$ ;  $dt=7$  m;  $mD=3$  m.

## Case studies

The developed system has been tested over large and various regions in order to evaluate its effectiveness and reliability for practical use. Test on both image and LiDAR data have been performed, considering both forest and agricultural applications. For each test area, the training and the validation were performed using the land use map and ground references provided by the Autonomous Province of Trento (Italy). The confusion matrix, the overall accuracy and the Kappa coefficient were considered as validation metrics for the classification maps, while the  $R^2$  and the RMSE were used for the forest attributes estimation. In the following section, some of the most significant results achieved on the study areas will be presented.

### *Agriculture Module - Image classification*

The Agriculture Module has been tested on an area located in the Adige Valley, in the

municipality of Aldeno, Trento. The area has an extension of 4 km<sup>2</sup> and the main visible crops are grapes, apples and pears, with some field of grasslands and other minor cultivations. Eight different classes were considered in the classification experiment (see Fig. 6). The used ortho-images are derived from the AGEA acquisition campaign over the whole province of Trento in July 2011. These aerial images were acquired at a relative flying height of 5000 m, and they were ortho-rectified on an already available (LiDAR derived) DTM. The final ortho-images have a 50 cm GSD.

The classifier was trained using small regions equally distributed on the whole area. The regions were chosen in order to be representative of the class variability inside the study area. The total number of training samples represents less than 0.35%.

58 features were selected by the feature selection module. These achieved results (Fig. 6) were provided by the SVM classifier on image classification: this algorithm has shown to overcome the other implemented classifiers. The post-processing was performed using a spatial filtering adopting a moving window of 9 by 9 pixels to filter the noise generated by the classification.

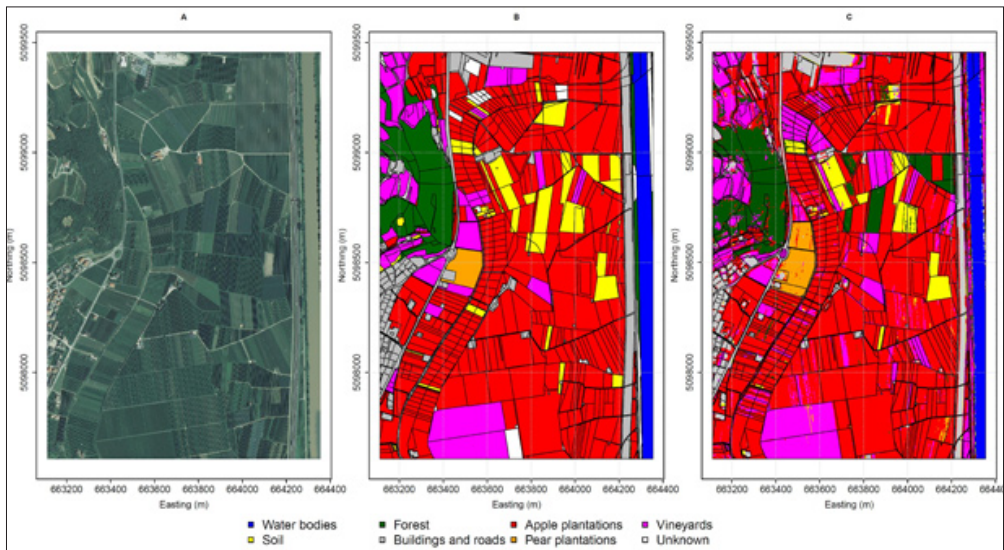


**Figure 6 - (a) Ortho-image of Dataset 1 (b) Ground reference (land use map). (c) Achieved classification on Dataset 1.**

From a visual comparison of the land use ground reference (Fig. 6b), the developed system succeeded in the classification of most of the crops (Fig. 6c). Note that Figure 6b refers to the field measurements carried out 2 years before the flight (i.e. 2009). Reports of field checks performed in 2011 confirmed that the wrongly classified areas have changed their land-use and thus the achieved classification results on these areas are actually correct. The classifier was successful in the separation of vineyards, apples and pears, even if all these plantations have rows that are very similar among each other. In this case, the small differences of the foliage spectral values together with the different size of the rows and the



crowns enabled to discriminate these plantations, showing the effectiveness of the selected features. The selection of training areas over two or more plantation lines have shown to provide better results in the distinction of vineyards, apples and pears classes, thanks to the geometrical features that clearly differ in these two classes. Residual misclassifications are mainly due to the seasonal changes of vegetation and their variability in spectral and geometrical information. Anyway, the classification statistics are very high as the overall accuracy on this test area is 97.6% and the Kappa Coefficient is 96.9% (Tab. 2).

**Table 2 - Number of pixels for each class used in the training and validation of the classifier and corresponding confusion matrix on the validation set.**

	Training	Validation	Water bodies	Soil	Forest	Buildings and roads	Apple plantations	Pear plantations	Vineyards	User's Accuracy (%)
Water bodies	6000	72914	72914	0	0	0	0	0	0	100.0
Soil	5680	9670	0	9456	0	0	130	0	0	98.6
Forest	5000	81537	0	17	75411	0	41	0	19	99.9
Buildings and roads	1740	27037	0	0	0	26451	0	0	0	100.0
Apple plantations	8000	191483	0	189	3125	586	190161	1092	2599	96.2
Pear plantations	2800	25172	0	0	0	0	26	24031	22	99.8
Vineyards	4720	97185	0	8	3001	0	1125	49	94545	95.8
Producer's accuracy (%)				100.0	97.8	92.5	97.8	99.3	95.5	97.3

### **Forest Module - Tree species classification**

The Forest Module has been tested on an area located in the municipality of Padergnone (Trento, Italy). The area has an extension of 1.75 km<sup>2</sup> and it is mainly dominated by broadleaves species (e.g. *Fagus sylvatica*, *Quercus ilex*) and *Pinus sylvestris*. 13 different classes were considered in the experiment. The classification was carried out using hyperspectral data having 65 bands and 1 m spatial resolution acquired in July 2008 with an AISA Eagle sensor.

25 bands out of 65 available were selected using the feature selection module (SFFS method with Jeffries-Matusita distance). The SVM classifier was trained using a training



set covering 0.26% of the image pixels and representative of every tree species present in the area. The achieved results are reported in Figure 7. The post-processing was performed using a spatial filtering: a moving window of 3 by 3 pixels was adopted to filter the noise generated by the classification.

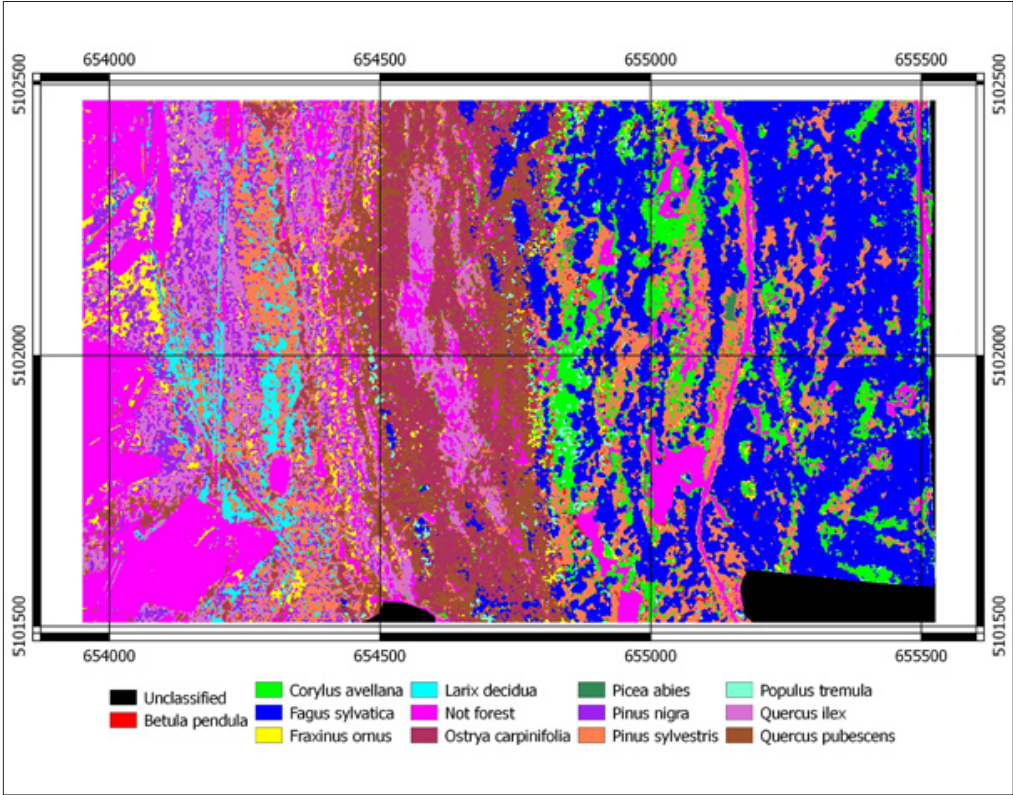


Figure 7 - Classification map of the Padergnone study area.

The classified map was validated on an independent validation set showing an overall accuracy of 93.3%, a kappa accuracy of 91.4%, and producer's accuracies ranging from 68.2% to 100% (see Tab. 3). Moreover the map was validated on the ground by technicians of the Forest Service of the Province of Trento, and the map was considered accurate enough to be used as reference for the Forest Inventory.

Compared to the previous case (section Module Agriculture - Image classification) no extra features were extracted, but only the original hyperspectral bands were used. The feature selection step is very fast (few minutes on a medium performance computer) while the classification step was slightly slower as it needs a tuning of the SVM parameters. Some classification maps were also generated with the maximum likelihood classifier and the k-NN classifier. These classifiers are much faster, but the classification accuracies were lower compared to the SVM ones.

**Table 3 - Confusion matrix and accuracies obtained for the classification of the tree species.**

	Betula pendula	Corylus avellana	Fagus sylvatica	Fraxinus ornus	Larix decidua	Not forest	Ostrya carpinifolia	Picea abies	Pinus nigra	Pinus sylvestris	Populus tremula	Quercus ilex	Quercus pubescens
Betula pendula	30	0	0	0	0	0	0	0	0	1	11	0	6
Corylus avellana	4	164	0	0	0	0	7	0	0	2	5	0	0
Fagus sylvatica	1	7	802	0	0	0	0	0	0	4	1	0	9
Fraxinus ornus	2	0	4	52	0	0	4	0	0	0	0	0	0
Larix decidua	0	0	0	0	101	0	0	0	0	21	0	0	0
Not forest	0	1	0	0	0	1392	0	0	0	4	0	9	0
Ostrya carpinifolia	0	0	1	0	0	0	90	0	0	0	0	0	16
Picea abies	0	0	0	0	0	0	0	67	0	0	0	0	0
Pinus nigra	0	0	0	0	2	0	0	0	119	18	0	13	0
Pinus sylvestris	0	0	2	0	8	0	1	2	12	328	3	0	4
Populus tremula	7	10	0	0	0	0	0	0	0	0	69	0	3
Quercus ilex	0	0	0	0	0	0	0	0	0	9	0	116	0
Quercus pubescens	0	0	6	6	0	0	21	0	0	0	0	0	95
N° pixels	44	182	815	58	111	1392	123	69	131	387	89	138	133
PA (%)	68.2	90.1	98.4	89.7	91.0	100.0	73.2	97.1	90.8	84.8	77.5	84.1	71.4
OA(%)	93.3												
KA(%)	91.4												

### Forest Module - Stem volume estimation

The test area is the same of the previous paragraph (Padergnone). In this case we used LiDAR data acquired in September 2007 with an Optech ALTM 3100EA sensor having a point density of about 10 points per square meter and up to 4 returns recorded. In-situ ground truth were considered for the validation of the results.

Individual tree crowns (ITCs; section Individual Tree Crowns (ITC) delineation) were delineated on the LiDAR data and LiDAR features were extracted from each ITC (section LiDAR features extraction). Out of all the variables extracted by the STEM plug-in only the following ones were used to train the SVR algorithm:  $H_{max}$ ,  $H_{mean}$ , Area,  $H_{q95}$ ,  $H_{cv}$ ,  $H_{q50}$ ,  $C_{q30}$ ,  $C_{q40}$ , and  $C_{q90}$ . The validation of the results carried out on a separate validation set showed a mean absolute error (MAE) of 0.17 m<sup>3</sup> and a root mean square error (RMSE) of 0.27 m<sup>3</sup>. Figure 8 shows the map of the stem volume at tree level obtained in the area considered.

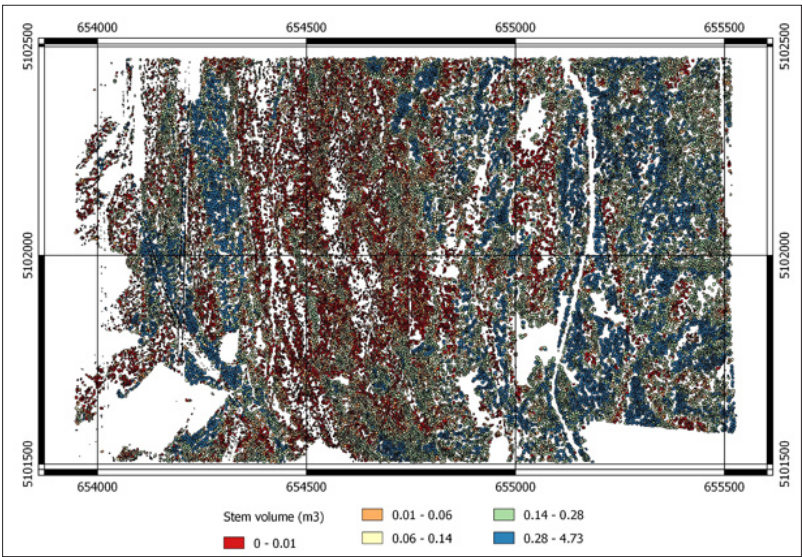


Figure 8 - Stem volume map at tree levels for the Padergnone study area.

**Forest Module - Forest structure classification**

The study area is the same of the two previous paragraphs (Padergnone). The area has been divided in tiles of 30 x 30 m size and the default parameter values have been adopted. The results are reported in Figure 9. The algorithm detected mostly single-layer forests, but many double-layer and multi-layers were detected too. The results were compared with 19 ground reference areas and the classification turned out to be correct on 17 of them.

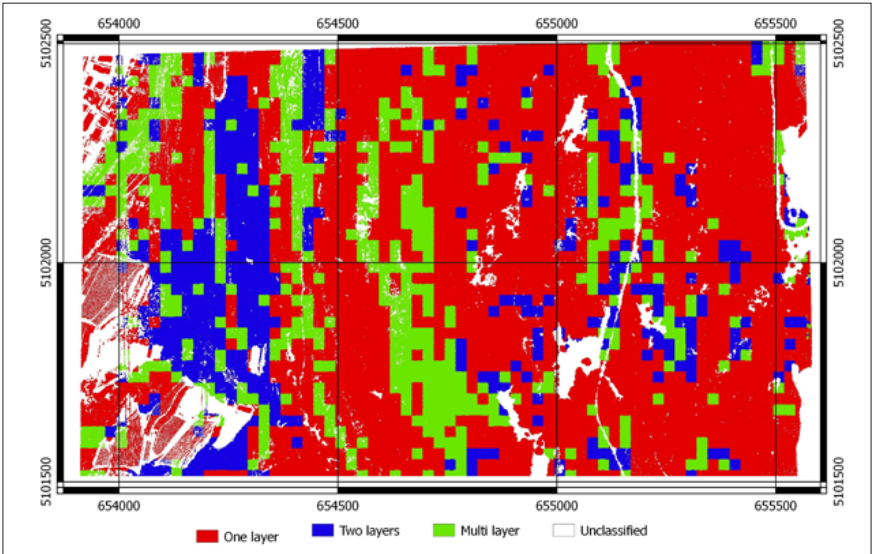


Figure 9 - Vertical forest structure results on Padergnone: one layer (red), two layers (blue) and multi-layer (green) structure have been detected by the algorithm.

## Conclusions and outlook

A free and open source plug-in for the efficient processing of remotely sensed data for crop and forest monitoring has been presented in this paper. The plug-in has been specifically conceived for Public Administrations providing a turn-key and straightforward processing workflow for unexperienced users. This instrument represents a novelty in the remote sensing domain, where tools that require specific expertise are usually available. Moreover, heterogeneous input data such as multi- and hyperspectral images as well as LiDAR data can be processed together in the same interface without the need to adopt many software or convert data in different formats.

The reduced number of options and limited computational time are essential in order to allow not-experienced users to use classification products for land administration purposes. On the other hand, the big variability of the monitored vegetation during the different months and the complexity to classify very similar crop species often using suboptimal data represented additional challenges of the project. These problems and the end-users requirements led to the development of supervised algorithms that exploit several features specifically optimized for these tasks. The processes can be run on a client-server service in order to reduce the computational time anymore, fulfilling the end-users requirements. Huge amount of data, over the whole province of Trento are expected to be collected and processed on dedicated clusters providing a practical answer to Public Administration needs.

The suitability of the proposed system has been demonstrated in the practical case studies presented in this paper. Most of the misclassification problems are in correspondence of “border-line” conditions, when the great variability of the data makes more difficult the automated classification process. In these cases, a visual interpretation of the data is still mandatory in order to deliver complete results.

The adopted 3D and 2D features have shown their effectiveness, at least in the Alpine area as they were conceived for the data processing in this area. Anyway, tests on different environments should be required to define the extendibility of the developed approach on other regions.

Most of the presented workflow has been realized using in-house research codes or already existing open source algorithms: the STEM QGIS plug-in (including the presented tool) is available for free download in the QGIS plug-in repository, being a new and valuable free instrument for many users as well as a starting framework to modify the existing tools and implement new functionalities.

The selection of effective training samples represents still the main limitation of this tool, when inexperienced users are supposed to work with. For this reason, a new tool to provide the position of candidate training areas will be developed in the future. The spectral information variability will be exploited to select these candidate regions with different cultivations, morphology and vegetation.

## Acknowledgements

The Authors would like to acknowledge the *Autonomous Province of Trento* and *TrentoRISE*, and in particular the Agriculture and Forests offices, for funding the STEM Project.

## References

- Altman N.S. (1992) - *An introduction to kernel and nearest-neighbor nonparametric regression*. The American Statistician, 46 (3): 175-185.
- Amadasun M., King R. (1989) - *Textural features corresponding to textural properties*.



- IEEE Transactions on Systems, Man, and Cybernetics, 19 (5), 1264-12741. doi: <http://dx.doi.org/10.1109/21.44046>.
- Bazi Y., Melgani F. (2006) - *Toward an Optimal SVM Classification System for Hyperspectral Remote Sensing Images*. IEEE Transaction on Geoscience and Remote Sensing, 44: 3374-3385. doi: <http://dx.doi.org/10.1109/TGRS.2006.880628>.
- Signal E. (1998) - *Using an ecological understanding of farmland to reconcile nature conservation requirements, EU agriculture policy and world trade agreements*. Journal of Applied Ecology, 35 (6): 949-954. doi: <http://dx.doi.org/10.1111/j.1365-2664.1998.tb00013.x>.
- Blaschke T. (2010) - *Object based image analysis for remote sensing*. ISPRS Journal of Photogrammetry and Remote Sensing, 65 (1): 2-16. doi: <http://dx.doi.org/10.1016/j.isprsjprs.2009.06.004>.
- Bouman C.A., Shapiro M. (1994) - *A Multiscale Random Field Model for Bayesian Image Segmentation*. IEEE Transaction on Image Processing, 3 (2). doi: <http://dx.doi.org/10.1109/83.277898>.
- Bruzzone L., Roli F., Serpico S.B. (1995) - *An extension of the Jeffreys-Matusita distance to multiclass cases for feature selection*. IEEE Transactions on Geoscience and Remote Sensing, 3 (6): 1318-1321. doi: <http://dx.doi.org/10.1109/36.477187>.
- Bruzzone L., Melgani F. (2005) - *Robust multiple estimator systems for the analysis of biophysical parameters from remotely sensed data*. IEEE Transactions on Geoscience and Remote Sensing, 43: 159-173. doi: <http://dx.doi.org/10.1109/TGRS.2004.839818>.
- Bruzzone L., Carlin L. (2006) - *A Multilevel Context-Based Sysyem for Classification of Very High Spatial Resolution Images*. IEEE Transactions on Geoscience and Remote Sensing, 44 (9): 2587-2600. doi: <http://dx.doi.org/10.1109/TGRS.2006.875360>.
- Clementel F., Colle G., Farruggia C., Floris A., Scrinzi G., Torresan C. (2012) - *Estimating forest timber volume by means of "low-cost" LiDAR data*. European Journal of Remote Sensing, 44: 125-140. doi: <http://dx.doi.org/10.5721/itjrs201244110>.
- Corona P., Cartisano R., Salvati R., Chirici G., Floris A., Martino P. Marchetti M., Scrinzi G., Clementel F., Travaglini D., Torresan C. (2012) - *Airborne Laser Scanning to support forest resource management under alpine, temperate and Mediterranean environments in Italy*. European Journal of Remote Sensing, 45: 27-37. doi: <http://dx.doi.org/10.5721/EuJRS20124503>.
- Dalponte M., Bruzzone L., Gianelle D. (2008) - *Fusion of hyperspectral and LIDAR remote sensing data for the classification of complex forest areas*. IEEE Transactions on Geoscience and Remote Sensing, 46 (5): 1416-1427. doi: <http://dx.doi.org/10.1109/TGRS.2008.916480>.
- Dalponte M., Bruzzone L., Vescovo L., Gianelle D. (2009) - *The role of spectral resolution and classifier complexity in the analysis of hyperspectral images of forest areas*. Remote Sensing and Environment, 113: 2345-2355. doi: <http://dx.doi.org/10.1016/j.rse.2009.06.013>.
- Dalponte M., Bruzzone L., Gianelle D. (2011) - *A system for the estimation of single-tree stem diameter and volume using multireturn LIDAR data*. IEEE Transactions on Geoscience and Remote Sensing, 49: 2479-2490. doi: <http://dx.doi.org/10.1109/TGRS.2011.2107744>.
- Dalponte M., Bruzzone L., Gianelle D. (2012) - *Tree species classification in the Southern*

- Alps based on the fusion of very high geometrical resolution multispectral/hyperspectral images and LiDAR data.* Remote Sensing and Environment, 123: 258-270. doi: <http://dx.doi.org/10.1016/j.rse.2012.03.013>.
- Haralick R.M., Shanmugam K., Dinstein I. (1973) - *Textural features for image classification.* IEEE Transactions on Systems, Man, and Cybernetics, SMC-3 (6): 610-621. doi: <http://dx.doi.org/10.1109/TSMC.1973.4309314>.
- Haralick R. (1979) - *Statistical and structural approaches to texture.* Proceedings of the IEEE, 67 (5): 786-804. doi: <http://dx.doi.org/10.1109/PROC.1979.11328>.
- Helmholz P., Rottensteiner F., Heipke C. (2014) - *Semi-Automatic verification of cropland and grassland using very high resolution mono-temporal satellite images.* ISPRS Journal of Photogrammetry and Remote Sensing, 97: 204-218. doi: <http://dx.doi.org/10.1016/j.isprsjprs.2014.09.008>.
- Hilker T., Wulder M.A., Coops N.C., Gougeon F.A., Heinzel J., Koch B., Clark M., Roberts D., Clark D., Hall R.J., Skakun R.S., Arsenault E.J., Case B.S., Leckie D.G., Tinis S., Nelson T., Burnett C., Cloney E., Paradine D., Hill D., Quinn R., Armstrong L., Shreenan R., Walsworth N. (2005) - *Issues in species classification of trees in old growth conifer stands.* Remote Sensing of Environment, 31: 175-190.
- Hoffbeck J.P., Landgrebe D.A. (1996) - *Classification of Remote Sensing Images Having High Spectral Resolution.* Remote Sensing of Environment, 57: 119-126. doi: [http://dx.doi.org/10.1016/0034-4257\(95\)00138-7](http://dx.doi.org/10.1016/0034-4257(95)00138-7).
- Kimes D.S., Ranson K.J., Sun G., Blair J.B. (2006) - *Predicting lidar measured forest vertical structure from multi-angle spectral data.* Remote Sensing of Environment, 100: 503-511. doi: <http://dx.doi.org/10.1016/j.rse.2005.11.004>.
- Kruse F.A., Lefkoff A.B., Boardman J.B., Heidebrecht K.B., Shapiro A.T., Barloon P.J., Goetz A.F.H. (1993) - *The Spectral Image Processing System (SIPS) - Interactive Visualization and Analysis of Imaging spectrometer Data.* Remote Sensing of Environment, 44: 145-163. doi: [http://dx.doi.org/10.1016/0034-4257\(93\)90013-N](http://dx.doi.org/10.1016/0034-4257(93)90013-N).
- Melgani F., Bruzzone L. (2004) - *Classification of hyperspectral remote sensing images with support vector machines.* IEEE Transactions on Geoscience and Remote Sensing, 42: 1778-1790. doi: <http://dx.doi.org/10.1109/TGRS.2004.831865>.
- Næsset E., Gobakken T., Bollandsås O.M., Gregoire T.G., Nelson R., Ståhl G. (2013) - *Comparison of precision of biomass estimates in regional field sample surveys and airborne LiDAR-assisted surveys in Hedmark County, Norway.* Remote Sensing of Environment, 130: 108-120. doi: <http://dx.doi.org/10.1016/j.rse.2012.11.010>.
- Nemmour H., Chibani Y. (2006) - *Multiple support vector machines for land cover change detection: an application for mapping urban extensions.* ISPRS Journal of Photogrammetry and Remote Sensing, 61: 125-133. doi: <http://dx.doi.org/10.1016/j.isprsjprs.2006.09.004>.
- Neteler M., Bowman M.H., Landa M., Metz M. (2012) - *GRASS-GIS: a multi-purpose open source GIS.* Environmental Modelling and Software, 31: 124-130. doi: <http://dx.doi.org/10.1016/j.envsoft.2011.11.014>.
- Peled A., Gilichinsky M. (2010) - *Knowledge-based classification of land cover for the quality assessment of GIS database.* The International Archives of the Photogrammetry, Remote Sensing and Spatial Information Sciences, 38 (4-8-2-W9): 217-222.
- Pirotti F., Grigolato S., Lingua E., Sitzia T., Tarolli P. (2012) - *Laser Scanner Applications*



- in Forest and Environmental Sciences*. Italian Journal of Remote Sensing, 44 (1): 109-123. doi: <http://dx.doi.org/10.5721/ItJRS20124419>.
- Pudil P., Novovičová J., Kittler J. (1994) - *Floating search methods in feature selection*. Pattern Recognition Letters, 15 (11): 1119-1125. doi: [http://dx.doi.org/10.1016/0167-8655\(94\)90127-9](http://dx.doi.org/10.1016/0167-8655(94)90127-9).
- Ruiz L.A., Recio J.A., Hermosilla T. (2007) - *Methods for automatic extraction of regularity patterns and its application to object-oriented image classification*. The International Archives of the Photogrammetry, Remote Sensing and Spatial Information Sciences, 36 (3/W49A5): 117-121.
- Shafri H.Z.M., Suhaili A., Mansor S. (2007) - *The Performance of Maximum Likelihood, Spectral Angle Mapper, Neural Network and Decision Tree Classifiers in Hyperspectral Image Analysis*. Journal of Computational Science, 3: 419-423. doi: <http://dx.doi.org/10.3844/jcssp.2007.419.423>.
- Shackelford A., Davis C.H. (2003) - *A Hierarchical Fuzzy Classification Approach for High-Resolution Multispectral Data Over Urban Areas*. IEEE Transactions on Geoscience and Remote Sensing, 41 (9): 1920-1932. doi: <http://dx.doi.org/10.1109/TGRS.2003.814627>.
- Sherill K.R., Lefsky M.A., Bradford J.B., Ryan M.G. (2008) - *Forest structure estimation and pattern exploration from discrete-return lidar in subalpine forests of the central Rockies*. Canadian Journal of Forest Resources, 38: 2081-2096. doi: <http://dx.doi.org/10.1139/X08-059>.
- Smola A.J., Schölkopf B. (2004) - *A tutorial on support vector regression*. Statistics and Computing, 14: 199-222. doi: <http://dx.doi.org/10.1023/B:STCO.0000035301.49549.88>.
- Trias-Sanz R. (2006) - *Texture orientation and period estimator between forests, orchards, vineyard, and tilled fields*. IEEE Transactions on Geoscience and Remote Sensing, 44 (10): 2755-2760. doi: <http://dx.doi.org/10.1109/TGRS.2006.875784>.
- Tsai C.A., Huang C.H., Chang C.W., Chen C.H. (2012) - *Recursive feature selection with significant variables of support vectors*. Computational and Mathematical Methods in Medicine, 2012 (712542). doi: <http://dx.doi.org/10.1155/2012/712542>.
- Vapnik V.N. (1999) - *The Nature of Statistical Learning Theory*. New York Berlin Heidelberg: Springer-Verlag.
- Warner T.A., Steinmaus K. (2005) - *Spatial classification of orchards and vineyards with high spatial resolution panchromatic imagery*. Photogrammetric Engineering & Remote Sensing, 71 (2): 179-187. doi: <http://dx.doi.org/10.14358/PERS.71.2.179>.
- Whitehurst A., Swatantran A., Blair J.B., Hofton M.A., Dubayah R. (2013) - *Characterization of Canopy Layering in Forested Ecosystems Using Full Waveform Lidar*. Remote Sensing, 5: 2014-2036. doi: <http://dx.doi.org/10.3390/rs5042014>.
- Zimble D.A., Evans D.L., Carlson G.C., Parker R.C., Grado S.C., Gerard P.D. (2003) - *Characterizing vertical forest structure using small-footprint airborne LiDAR*. Remote Sensing of Environment, 87: 171-182. doi: [http://dx.doi.org/10.1016/S0034-4257\(03\)00139-1](http://dx.doi.org/10.1016/S0034-4257(03)00139-1).